The Journal of Chemical Physics

A Fermi smearing variant of the Tamm–Dancoff approximation for nonadiabatic dynamics involving S_1–S_0 transitions: Validation and application to azobenzene

Cite as: J. Chem. Phys. **153**, 094104 (2020); https://doi.org/10.1063/5.0016487
Submitted: 04 June 2020 . Accepted: 12 August 2020 . Published Online: 02 September 2020

Laurens D. M. Peters, Jörg Kussmann, and Christian Ochsenfeld

The Journal of Chemical Physics ARTICLE scitation.org/journal/jcp

A Fermi smearing variant of the Tamm–Dancoff approximation for nonadiabatic dynamics involving S_1–S_0 transitions: Validation and application to azobenzene

Cite as: J. Chem. Phys. 153, 094104 (2020); doi: 10.1063/5.0016487
Submitted: 4 June 2020 • Accepted: 12 August 2020 •
Published Online: 2 September 2020

Laurens D. M. Peters,[1] Jörg Kussmann,[1] and Christian Ochsenfeld[1,2,a)]

AFFILIATIONS

[1]Chair of Theoretical Chemistry, Department of Chemistry, University of Munich (LMU), Butenandtstr. 7, D-81377 München, Germany
[2]Max Planck Institute for Solid State Research, Heisenbergstr. 1, D-70569 Stuttgart, Germany

[a)]Author to whom correspondence should be addressed: c.ochsenfeld@fkf.mpg.de

ABSTRACT

The main shortcoming of time-dependent density functional theory (TDDFT) regarding its use for nonadiabatic molecular dynamics (NAMD) is its incapability to describe conical intersections involving the ground state. To overcome this problem, we combine Fermi smearing (FS) DFT with a fractional-occupation variant of the Tamm–Dancoff approximation (TDA) of TDDFT in the generalized gradient approximation. The resulting method (which we denote as FS-TDA) gives access to ground- and excited-state energies, gradients, and nonadiabatic coupling vectors, which are physically correct even in the vicinity of S_1–S_0 conical intersections. This is shown for azobenzene, a widely used photoswitch, via single point calculations and NAMD simulations of its *cis–trans* photoisomerization. We conclude that FS-TDA may be used as an efficient alternative to investigate these processes.

I. INTRODUCTION

Time-dependent density functional theory (TDDFT)[1–3] can be regarded as the workhorse of today's theoretical photochemistry.[4] Being computationally less demanding than the other methods, it gives access to excitation spectra,[5,6] excited-state properties,[7,8] and even nonadiabatic molecular dynamics (NAMD)[9–14] of good quality even for large molecular systems. Despite TDDFT's increasing popularity, e.g., in the fields of photoswitches[15,16] or photoactive proteins,[17–19] its scope of application is limited. For example, the correct description of conical intersections involving the ground state is not possible[3,20–22] due to the single-reference nature of TDDFT.

Many different approaches have been introduced to tackle this problem. It was, for example, shown that the Tamm–Dancoff approximation (TDA)[23] improves upon TDDFT regarding the stability of NAMD.[13,24] Teh and Subotnik were able to demonstrate that including one doubly excited configuration yields the correct physical description around S_1–S_0 conical intersections.[25] Similar results can be obtained by introducing artificial couplings between ground and singly excited states.[26,27] Computationally more demanding approaches are spin-flip TDDFT,[28–30] combining DFT with a multireference method,[31–33] or calculating the electronic structure as an ensemble of densities or states.[34,35] Practical approaches of the latter are thermal DFT,[36,37] restricted-ensemble Kohn–Sham (KS) DFT,[38–41] or thermally assisted-occupation (TAO) DFT.[42–45] For a recent review of emerging DFT methods tackling orbital degeneracy, the reader is referred to Ref. 46.

In this work, we want to introduce a different approach for an efficient calculation of S_1–S_0 transitions that we denote as Fermi smearing TDA (FS-TDA). To guarantee the convergence of DFT calculations even close to the conical intersection, we use Fermi smearing.[47] This involves a fictitious electronic

temperature (T) which leads to fractional occupation numbers (n). A similar ansatz is made in the floating occupation molecular orbital-complete active space configuration interaction method[48–50] in the realm of the Hartree–Fock or semi-empirical methods. In contrast to previous works based on DFT (e.g., TAO-DFT[42–45]), we solely use n to converge our ground-state calculations applying a constant T, while the exchange-correlation functional does not explicitly depend on the occupation numbers n. Excited-state energies and properties are obtained from a subsequent TDA-TDDFT calculation, which accounts for the fractional occupation numbers of the ground-state configuration without requiring derivatives with respect to n.

We start with a brief summary of the theory in Sec. II, where we additionally use a two-orbital system (HeH^+ with a minimal basis) to validate our approach and to discuss the effect of the electronic temperature on the excited states. In Sec. III, we apply FS-TDA to azobenzene, a prominent photoswitch, whose derivatives can be found, e.g., in photopharmaceuticals.[16,51–53] We compare FS-TDA energies and properties to the results of complete active space self-consistent field (CASSCF)[54] and complete active space second order perturbation theory (CASPT2)[55–58] calculations and evaluate NAMD simulations combining FS-TDA with trajectory surface hopping.[59,60] Section IV presents our conclusions and gives an outlook. Computational details are listed in the supplementary material.

II. THEORY

Throughout this work, i, j, k, ... denote occupied, a, b, c, ... denote virtual, and p, q, r denote arbitrary molecular orbitals (MOs). μ, ν, κ and I, J, ... represent atomic orbitals (AOs) and electronic states, respectively. We restrict ourselves to pure functionals without exact exchange.

Close to a conical intersection involving the ground state, the highest occupied MO (HOMO) and the lowest unoccupied MO (LUMO) are nearly degenerate, leading to non-converging self-consistent field (SCF) calculations. Nonetheless, KS-DFT can be converged, when Fermi smearing[47] is applied,

$$n_p = \frac{1}{1+\exp\left[\dfrac{\epsilon_p - \epsilon_\mathrm{F}}{k_\mathrm{B}T}\right]}, \tag{1}$$

resulting in a partial occupation ($0 < n_p < 1$) and, thus, optimization of virtual MOs. ϵ_p is the orbital energy, ϵ_F is the Fermi level, and k_B is the Boltzmann constant. T is the absolute electronic temperature used to generate fractional occupation numbers and should not be confused with the "real" temperature involved in MD or thermodynamics. The occupation of a virtual orbital (n_a) is, thus, increasing with a decreasing HOMO–LUMO gap and increasing T (see Fig. S1 of the supplementary material). Since the resulting ground state is represented by an ensemble density, the calculation of ground-state forces also requires a slight modification of the Pulay force term.[61]

In order to calculate excitations, we follow the procedure of Yang *et al.*[62] and define the so-called Fermi-space (see Fig. 1). Orbitals within this space are fractionally occupied and, thus, belong to both the occupied space and the virtual space. This has two major effects on the following TDA calculation. First, the two-electron integrals and the second order exchange-correlation functional derivatives (f^{xc}_{iajb}) need to be rescaled[62] with $\sqrt{n_i}$ or $\sqrt{1-n_a}$, leading to the FS-TDA equations,

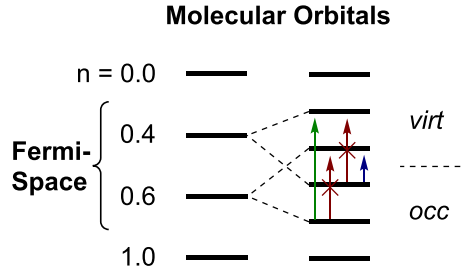

FIG. 1. Concept of FS-TDA: Molecular orbitals with a fractional occupation number ($0 < n < 1$) are regarded as both occupied and virtual. Within the Fermi-space, we can distinguish excitations with a positive excitation energy (leftmost, green arrow, $\epsilon_a - \epsilon_i > 0$), excitations with a negative excitation energy (rightmost, blue arrow, $\epsilon_a - \epsilon_i < 0$), and redundant excitations with zero excitation energy (middle, red arrows, $\epsilon_a - \epsilon_i = 0$). The latter need to be neglected during the calculation. Please note that the orbitals in the right column are, in contrast to the left column, not ordered by their energy.

$$\tilde{\mathbf{A}}\tilde{\mathbf{X}}_I = \tilde{\omega}_I\tilde{\mathbf{X}}_I, \tag{2}$$

with

$$\begin{aligned}\tilde{A}_{iajb} &= \delta_{ij}\delta_{ab}(\epsilon_a - \epsilon_i) + \tilde{D}_{ijab},\\ \tilde{D}_{ijab} &= [(ia|jb) + f^{\mathrm{xc}}_{iajb}] \times \sqrt{n_i(1-n_a)n_j(1-n_b)}.\end{aligned} \tag{3}$$

Second, redundant and negative excitations may occur when solving Eq. (2) (see Fig. 1). Redundant excitations are neglected by setting the corresponding elements of the transition density ($\tilde{X}^I_{ia}$) to zero. ω_1 is defined as the first positive, non-redundant excitation ($\omega_I > 10^{-6}$). Please note that the occurrence of negative excitations makes the use of TDDFT without TDA or additional restrictions impossible, as this leads to imaginary excitation energies.

Equations for the FS-TDA excited-state gradients ($\tilde{\boldsymbol{\omega}}^{\mathrm{x}}_I$)[7] and nonadiabatic coupling vectors ($\tilde{\boldsymbol{\tau}}_{0I}$,[8] with electron translational factors[63]) can be derived using the Lagrangian method with Eq. (2) instead of the standard TDA equation,

$$\begin{aligned}\tilde{\boldsymbol{\omega}}^{\mathrm{x}}_I = &\sum_{\mu\nu}\{h^{\mathrm{x}}_{\mu\nu}P^I_{\mu\nu} - S^{\mathrm{x}}_{\mu\nu}W^I_{\mu\nu} + v^{\mathrm{xc(x)}}_{\mu\nu}P^I_{\mu\nu}\}\\ &+ \sum_{\mu\nu\kappa\lambda}(\mu\nu|\kappa\lambda)^{\mathrm{x}}P^I_{\mu\nu}P_{\kappa\lambda} + \sum_{\mu\nu\kappa\lambda}\tilde{D}^{\mathrm{x}}_{\mu\nu\kappa\lambda}\tilde{X}^I_{\mu\nu}\tilde{X}^I_{\kappa\lambda},\end{aligned} \tag{4}$$

$$\begin{aligned}\tilde{\boldsymbol{\tau}}_{0I} = &\sum_{\mu\nu}[h^{\mathrm{x}}_{\mu\nu}P^{0I}_{\mu\nu} - S^{\mathrm{x}}_{\mu\nu}W^{0I}_{\mu\nu} + v^{\mathrm{xc\,(x)}}_{\mu\nu}P^{0I}_{\mu\nu}]\\ &+ \sum_{\mu\nu\kappa\lambda}(\mu\nu|\kappa\lambda)^{\mathrm{x}}P^{0I}_{\mu\nu}P_{\kappa\lambda},\end{aligned} \tag{5}$$

where $\mathbf{h}$ is the one-electron core Hamiltonian matrix, $\mathbf{S}$ is the overlap matrix, $\mathbf{v}_{\mathrm{xc}}$ is the first order exchange-correlation functional derivative, and $\mathbf{P}$ is the ground-state density. For the sake of simplicity,

we use the same symbols for matrices in the MO and AO space but different indices (e.g., $\tilde{X}^I_{\mu\nu}$ and $\tilde{X}^I_{ia}$).

The relaxed difference density matrix of the excited-state gradient ($\mathbf{P}_I$) consists of an unrelaxed contribution ($\mathbf{T}_I$) and the Z-vector ($\mathbf{Z}_I$),

$$\mathbf{P}_I = \mathbf{T}_I + \mathbf{Z}_I. \tag{6}$$

The latter is obtained by solving the Z-vector equation,

$$\sum_{jb} \tilde{A}_{ijab} Z^I_{jb} = -(Q^I_{ia} - Q^I_{ai}). \tag{7}$$

The equations for $\mathbf{T}_I$ and the right-hand side ($\mathbf{Q}_I$) can be found in the supplementary material. Just as in the FS-TDA equations, contributions from redundant excitation are neglected by setting the corresponding elements of $\mathbf{Z}_I$ and $\mathbf{Q}_I$ to zero. This ensures that the excitation does not lead to a gain or a loss of electrons,

$$\sum_{\mu\nu} P^I_{\mu\nu} S_{\mu\nu} = 0. \tag{8}$$

This does not hold for the energy-weighted difference density matrix ($\mathbf{W}_I$) for which the equations and their derivations are given in the supplementary material. Here, the redundant elements of $\mathbf{Q}_I$ need to be considered.

In Fig. S2 of the supplementary material, we show that numerical and analytical gradients of the S_1 state of HeH^+ are in good agreement for different Ts and bond lengths. The small errors can be explained by the fact that we neglect the change of n_p during the perturbation (x) in our analytical derivative. Additionally, we have conducted an analysis of the change of the matrix elements of $\mathbf{P}$, $\mathbf{T}_1$, $\mathbf{Z}_1$, and $\mathbf{P}_1$ of HeH^+ with increasing temperature (see Fig. S3 of the supplementary material). While $\mathbf{T}_1$ is nearly constant, $\mathbf{P}$ and $\mathbf{Z}_1$ change substantially with T (see Fig. 2). $\mathbf{P}$ becomes equally distributed onto both atoms due to the increasing occupation of the LUMO. $\mathbf{Z}_1$ becomes zero, as the optimization of the LUMO during the SCF reduces the amount of relaxation in the excited-state density. Both observations are, thus, in agreement with what we expect from a step-wise occupation of the LUMO.

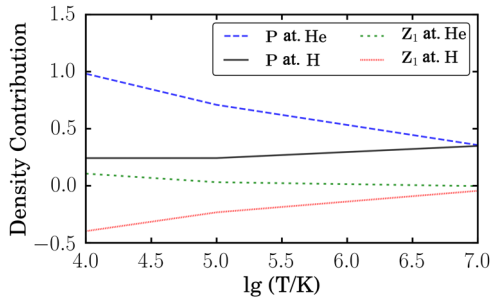

FIG. 2. Change of the ground-state density ($\mathbf{P}$) and the Z-vector ($\mathbf{Z}_1$) of HeH^+ located at different atoms with the electronic temperature. Values for H and He were obtained from a FS-TDA (PBE/STO-3G) calculation as $D_{\mu\mu} + \frac{1}{2}(D_{\mu\nu} + D_{\nu\mu})$, with μ/ν being the s-orbital at H/He and He/H, respectively. A minimal basis has been chosen to obtain a two-orbital system.

Solving the Z-vector equation is not necessary in the case of the nonadiabatic coupling vectors including the ground state.[8] As the relaxed difference density ($\mathbf{P}_{0I}$) is

$$\mathbf{P}_{0I} = \frac{1}{\tilde{\omega}_I} \tilde{\mathbf{X}}_I, \tag{9}$$

redundant excitations do not affect their calculation nor the calculation of the energy-weighted difference density matrix ($\mathbf{W}_{0I}$) for which the calculation is again shown in the supplementary material. There, we also validate our ansatz by comparing analytical and numerical $\tilde{\boldsymbol{\tau}}_{0I}$'s.

III. ILLUSTRATIVE EXAMPLE: AZOBENZENE

As already mentioned above, azobenzene is a photoswitch converting light into molecular motion. Due to its promising applicability in, e.g., the treatment of cancer, it has been the target of many experimental[64] and theoretical[16,29,65,66] investigations. The excitation into the S_1 state has a $n \rightarrow \pi^*$ character (natural transition orbitals are shown in Fig. S5 of the supplementary material), which allows the molecule to rotate around the central N–N double bond leading to a *cis* → *trans* or a *trans* → *cis* isomerization. At a C–N–N–C dihedral of ~90°, azobenzene features a S_1–S_0 conical intersection, making it the ideal test for the introduced FS-TDA method implemented in the FermiONs++ program package.[67–69]

Comparing the electronic structure of FS-TDA and the state-averaged CASSCF near the conical intersection (see Fig. S4 of the supplementary material) reveals that the weights of the double occupied states [$n(2)$ and $\pi^*(2)$] calculated with the CASSCF are nearly equivalent to the occupation numbers of corresponding orbitals calculated with DFT at an electronic temperature of 300 K. The character of the S_1 state is also similar as the CASSCF $n(1)$ $\pi^*(1)$ state is generated by FS-TDA via a linear combination of the positive $n \rightarrow \pi^*$ and the negative $\pi^* \rightarrow n$ excitation.

This observation is supported by the fact that FS-TDA excitation energies are in good agreement with CASSCF and CASPT2 calculations [see Fig. 3(a) and Fig. S6 of the supplementary material]. However, we observe three differences when comparing FS-TDA energies with CAS methods: (1) The excitation energies at the optimized *cis* and *trans* geometries are significantly smaller, (2) the rotational barrier is lower, and (3) the slope of the potential energy surface changes at a C–N–N–C dihedral of ~80°/100°. The reason for the first one is that we are so far restricted to generalized gradient approximation (GGA) functionals. In order to describe the charge-transfer character of the excitation more accurately, functionals with exact exchange or long-range-corrected functionals need to be applied (see, e.g., Ref. 70 for an extensive benchmark). This would also correct the rotational barrier. The last observation could be improved by applying a higher T (see Fig. S7 of the supplementary material). While this leads to a slightly smoother behavior of the excitation energies, it significantly lowers the rotational barrier. Because of this and the fact that increasing T leads to the appearance of rather unphysical excitations (e.g., HOMO − 1 → HOMO with both orbitals having an occupation of almost one), we choose

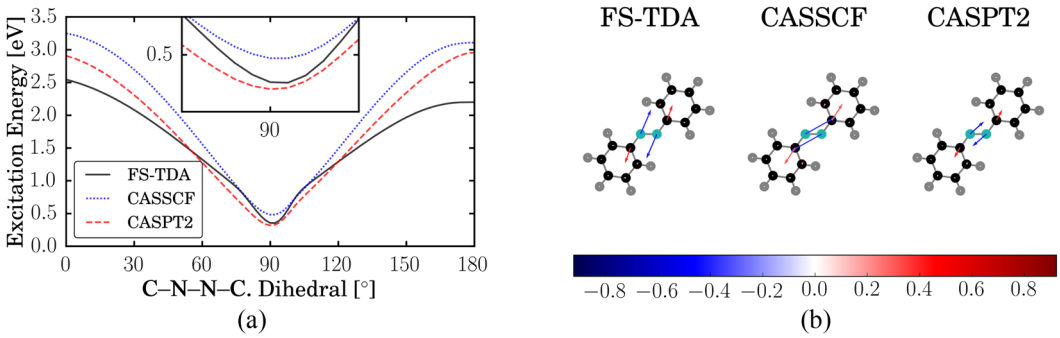

FIG. 3. (a) Excitation energies (ω_1) of the S_1 state of azobenzene during the *cis–trans* isomerization and (b) the difference between the S_1 and S_0 gradients ($\boldsymbol{\omega}_1^x$) of azobenzene with a C–N–N–C dihedral of 88° at the FS-TDA (PBE/def2-TZVP, Fermi temperature: 300 K), CASSCF/def2-TZVP, and CASPT2/def2-TZVP level of theory. The subplot of (a) shows an expanded view around 90°. In (b), the gradient vectors in atomic units were scaled with a factor of 40 before being plotted in the x–y plane. The colors of the arrows (see the color bar) reflect the components in the z direction.

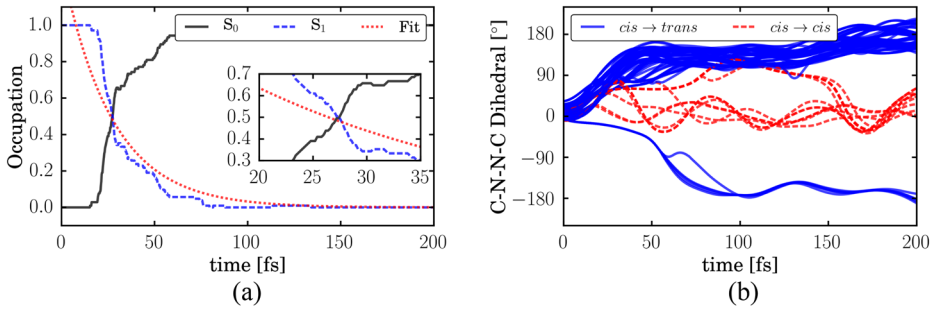

FIG. 4. Nonadiabatic molecular dynamics (NAMD) of azobenzene at the FS-TDA (PBE/def2-TZVP, Fermi temperature: 300 K) level of theory: Change of (a) the average state occupations and (b) the C–N–N–C dihedrals. In (a), we additionally show an exponential fit to the S_1 decay resulting in a lifetime of 35 fs. The subplot shows an expanded view around 27 fs. In (b), we distinguish between trajectories with successful (blue solid lines) and unsuccessful (red dashed lines) *cis–trans* isomerizations.

T as small as possible in this example. The excitation gradients of FS-TDA are compared to CASSCF and CASPT2 gradients in Fig. 3(b) and Figs. S8 and S9 of the supplementary material. FS-TDA shows, again, the right physical behavior while being significantly closer to the CASPT2 result than the CASSCF.

As a final test for FS-TDA, we conduct 105 NAMD trajectories of azobenzene starting from structures close to its *cis* form. In contrast to standard TDDFT, not a single trajectory died due to the convergence issues of the SCF or the TDDFT equations and most of the trajectories showed the expected *cis* → *trans* isomerization. The results are summarized in Fig. 4, where we present average state occupations and plot the change of the C–N–N–C dihedral during the trajectories. The determined lifetime is ~35 fs, which is significantly shorter than the CASSCF results (67 fs)[66] or the spin-flip TDDFT results (53 fs)[29] from the literature, while the quantum yield is larger (0.85 vs 0.67[66] or 0.34[29]). Both may be the result of the PBE functional leading to a low rotational barrier and a too steep S_1 potential energy surface due to its poor description of charge-transfer excitations. Similar to the CASSCF dynamics,[66] we observe *cis* → *trans* isomerizations in both directions. However, one direction is strongly favored as it involves less sterical hindrance during the rotation [see Fig. 4(b) and Ref. 66].

IV. CONCLUSION AND OUTLOOK

We have introduced the FS-TDA ansatz to perform excited-state calculations and dynamics at the TDDFT level using fractional occupation numbers. Static calculations of azobenzene have revealed that it yields the right physical description of the system even close to a S_1–S_0 conical intersections and when an electronic temperature of 300 K is applied, enabling NAMD simulations of its *cis* → *trans* isomerization. The latter shows the right isomerization mechanism and can be performed efficiently with the excited-state routines[15] of the FermiONs++ program package.[67–69] One trajectory takes only ~12 h on two Intel Xeon CPU E5 2640 v4 at 2.20 GHz (20 threads) central processing units (CPUs) and four AMD FirePro 3D W8100 graphics processing units (GPUs) using a triple-zeta basis. Further investigations should tackle the transferability to molecular systems involving radical transition states or triplet states and the use of more complex density functionals (exact-exchange or long-range-corrected functionals) to obtain better potential energy surfaces and dynamics. Additionally, the electronic temperature could be adjusted to improve the results. We conclude that FS-TDA dynamics might be an efficient and useful tool to study nonadiabatic processes involving S_1–S_0 transitions.

SUPPLEMENTARY MATERIAL

See the supplementary material for computational details, additional derivations, and supplementary plots of energies, occupation numbers, densities, gradients, and nonadiabatic coupling vectors.

ACKNOWLEDGMENTS

We dedicate this work to Professor Bernd Giese on the occasion of his 80th birthday. Financial support was provided by the Innovative Training Network "Computational Spectroscopy In Natural Sciences and Engineering" (ITN-COSINE) and the DFG Cluster of Excellence (EXC 2089) "e-conversion." C.O. acknowledges further support as Max-Planck-Fellow at the MPI-FKF Stuttgart.

DATA AVAILABILITY

The data that support the findings of this study are available within the article and its supplementary material.

REFERENCES

[1] M. E. Casida, in *Recent Advances in Density Functional Methods*, edited by D. P. Chong (World Scientific, 1995), pp. 155–192.
[2] M. E. Casida, J. Mol. Struct.: THEOCHEM **914**, 3 (2009).
[3] M. E. Casida and M. Huix-Rotllant, Annu. Rev. Phys. Chem. **63**, 287 (2012).
[4] A. Dreuw, ChemPhysChem **7**, 2259 (2006).
[5] A. Dreuw and M. Head-Gordon, Chem. Rev. **105**, 4009 (2005).
[6] A. D. Laurent and D. Jacquemin, Int. J. Quantum Chem. **113**, 2019 (2013).
[7] F. Furche and R. Ahlrichs, J. Chem. Phys. **117**, 7433 (2002).
[8] R. Send and F. Furche, J. Chem. Phys. **132**, 044107 (2010).
[9] I. Tavernelli, E. Tapavicza, and U. Rothlisberger, J. Mol. Struct.: THEOCHEM **914**, 22 (2009).
[10] E. Tapavicza, I. Tavernelli, and U. Rothlisberger, Phys. Rev. Lett. **98**, 023001 (2007).
[11] E. Tapavicza, I. Tavernelli, U. Rothlisberger, C. Filippi, and M. E. Casida, J. Chem. Phys. **129**, 124108 (2008).
[12] M. Casida, B. Natarajan, and T. Deutsch, *Fundamentals of Time-Dependent Density Functional Theory* (Springer, Berlin, Heidelberg, 2014), Vol. 837, pp. 279–299.
[13] E. Tapavicza, G. D. Bellchambers, J. C. Vincent, and F. Furche, Phys. Chem. Chem. Phys. **15**, 18336 (2013).
[14] B. F. E. Curchod, A. Sisto, and T. J. Martínez, J. Phys. Chem. A **121**, 265 (2017).
[15] L. D. M. Peters, J. Kussmann, and C. Ochsenfeld, J. Chem. Theory Comput. **15**, 6647 (2019).
[16] D. B. Konrad, G. Savasci, L. Allmendinger, D. Trauner, C. Ochsenfeld, and A. M. Ali, J. Am. Chem. Soc. **142**, 6538 (2020).
[17] R. Liang, F. Liu, and T. J. Martínez, J. Phys. Chem. Lett. **10**, 2862 (2019).
[18] J. K. Yu, R. Liang, F. Liu, and T. J. Martínez, J. Am. Chem. Soc. **141**, 18193 (2019).
[19] L. D. M. Peters, J. Kussmann, and C. Ochsenfeld, J. Phys. Chem. Lett. **11**, 3955 (2020).
[20] B. G. Levine, C. Ko, J. Quenneville, and T. J. MartÍnez, Mol. Phys. **104**, 1039 (2006).
[21] M. E. Casida, F. Gutierrez, J. Guan, F.-X. Gadea, D. Salahub, and J.-P. Daudey, J. Chem. Phys. **113**, 7062 (2000).
[22] S. Gozem, F. Melaccio, A. Valentini, M. Filatov, M. Huix-Rotllant, N. Ferré, L. M. Frutos, C. Angeli, A. I. Krylov, A. A. Granovsky, R. Lindh, and M. Olivucci, J. Chem. Theory Comput. **10**, 3074 (2014).
[23] S. Hirata and M. Head-Gordon, Chem. Phys. Lett. **314**, 291 (1999).
[24] F. Cordova, L. J. Doriol, A. Ipatov, M. E. Casida, C. Filippi, and A. Vela, J. Chem. Phys. **127**, 164111 (2007).
[25] H.-H. Teh and J. E. Subotnik, J. Phys. Chem. Lett. **10**, 3426 (2019).
[26] S. L. Li, A. V. Marenich, X. Xu, and D. G. Truhlar, J. Phys. Chem. Lett. **5**, 322 (2014).
[27] Y. Shu, K. A. Parker, and D. G. Truhlar, J. Phys. Chem. Lett. **8**, 2107 (2017).
[28] Y. Shao, M. Head-Gordon, and A. I. Krylov, J. Chem. Phys. **118**, 4807 (2003).
[29] L. Yue, Y. Liu, and C. Zhu, Phys. Chem. Chem. Phys. **20**, 24123 (2018).
[30] E. Salazar and S. Faraji, Mol. Phys. **2020**, e1764120.
[31] J. Gräfenstein and D. Cremer, Mol. Phys. **103**, 279 (2005).
[32] S. Grimme and M. Waletzke, J. Chem. Phys. **111**, 5645 (1999).
[33] L. Gagliardi, D. G. Truhlar, G. Li Manni, R. K. Carlson, C. E. Hoyer, and J. L. Bao, Acc. Chem. Res. **50**, 66 (2017).
[34] M. Levy, Phys. Rev. A **26**, 1200 (1982).
[35] E. H. Lieb, Int. J. Quantum Chem. **24**, 243 (1983).
[36] A. Pribram-Jones, S. Pittalis, E. Gross, and K. Burke, *Frontiers and Challenges in Warm Dense Matter* (Springer, Cham, 2014), Vol. 96, pp. 25–60.
[37] A. Pribram-Jones, P. E. Grabowski, and K. Burke, Phys. Rev. Lett. **116**, 233001 (2016).
[38] M. Filatov and S. Shaik, Chem. Phys. Lett. **304**, 429 (1999).
[39] M. Filatov, F. Liu, and T. J. Martínez, J. Chem. Phys. **147**, 034113 (2017).
[40] M. Filatov, S. K. Min, and K. S. Kim, J. Chem. Theory Comput. **14**, 4499 (2018).
[41] T. Kowalczyk, T. Tsuchimochi, P.-T. Chen, L. Top, and T. Van Voorhis, J. Chem. Phys. **138**, 164101 (2013).
[42] J. D. Chai, J. Chem. Phys. **136**, 161101 (2012).
[43] J. D. Chai, J. Chem. Phys. **140**, 18A512 (2014).
[44] J. D. Chai, J. Chem. Phys. **146**, 234106 (2017).
[45] C.-Y. Lin, K. Hui, J.-H. Chung, and J.-D. Chai, RSC Adv. **7**, 50496 (2017).
[46] E. S. F. Maroto and J. C. Sancho-García, Computation **7**, 62 (2019).
[47] N. D. Mermin, Phys. Rev. **137**, A1441 (1965).
[48] G. Granucci and A. Toniolo, Chem. Phys. Lett. **325**, 79 (2000).
[49] P. Slavíček and T. J. Martínez, J. Chem. Phys. **132**, 234102 (2010).
[50] E. G. Hohenstein, M. E. F. Bouduban, C. Song, N. Luehr, I. S. Ufimtsev, and T. J. Martínez, J. Chem. Phys. **143**, 014111 (2015).
[51] A. A. Beharry and G. A. Woolley, Chem. Soc. Rev. **40**, 4422 (2011).
[52] J. Broichhagen, J. A. Frank, and D. Trauner, Acc. Chem. Res. **48**, 1947 (2015).
[53] L. Dong, Y. Feng, L. Wang, and W. Feng, Chem. Soc. Rev. **47**, 7339 (2018).
[54] B. Roos, Chem. Phys. Lett. **15**, 153 (1972).
[55] K. Andersson, P. Å. Malmqvist, B. O. Roos, A. J. Sadlej, and K. Wolinski, J. Phys. Chem. **94**, 5483 (1990).
[56] K. Andersson, P. Å. Malmqvist, and B. O. Roos, J. Chem. Phys. **96**, 1218 (1992).
[57] C. Angeli, R. Cimiraglia, S. Evangelisti, T. Leininger, and J.-P. Malrieu, J. Chem. Phys. **114**, 10252 (2001).
[58] C. Angeli, S. Borini, M. Cestari, and R. Cimiraglia, J. Chem. Phys. **121**, 4043 (2004).
[59] S. Hammes-Schiffer and J. C. Tully, J. Chem. Phys. **101**, 4657 (1994).
[60] J. C. Tully, J. Chem. Phys. **93**, 1061 (1990).
[61] A. M. N. Niklasson, J. Chem. Phys. **129**, 244107 (2008).
[62] W. Yang, P. Mori-Sánchez, and A. J. Cohen, J. Chem. Phys. **139**, 104114 (2013).
[63] S. Fatehi, E. Alguire, Y. Shao, and J. E. Subotnik, J. Chem. Phys. **135**, 234105 (2011).
[64] H. M. D. Bandara and S. C. Burdette, Chem. Soc. Rev. **41**, 1809 (2012).
[65] G. Granucci and M. Persico, Theor. Chem. Acc. **117**, 1131 (2007).
[66] M. Pederzoli, J. Pittner, M. Barbatti, and H. Lischka, J. Phys. Chem. A **115**, 11136 (2011).
[67] J. Kussmann and C. Ochsenfeld, J. Chem. Phys. **138**, 134114 (2013).
[68] J. Kussmann and C. Ochsenfeld, J. Chem. Theory Comput. **11**, 918 (2015).
[69] J. Kussmann and C. Ochsenfeld, J. Chem. Theory Comput. **13**, 3153 (2017).
[70] D. Jacquemin, V. Wathelet, E. A. Perpète, and C. Adamo, J. Chem. Theory Comput. **5**, 2420 (2009).